

Investigating the Effect of Power Curtailment on the Switch of a Solar Boost Converter Under Residential Loads

Alpizar Castillo, Joel; Engström, Carina; Ramirez Elizondo, Laura; Bauer, Pavol

DOI

[10.1109/PEMC61721.2024.10726347](https://doi.org/10.1109/PEMC61721.2024.10726347)

Publication date

2024

Document Version

Final published version

Published in

Proceedings of the 2024 IEEE 21st International Power Electronics and Motion Control Conference (PEMC)

Citation (APA)

Alpizar Castillo, J., Engström, C., Ramirez Elizondo, L., & Bauer, P. (2024). Investigating the Effect of Power Curtailment on the Switch of a Solar Boost Converter Under Residential Loads. In *Proceedings of the 2024 IEEE 21st International Power Electronics and Motion Control Conference (PEMC)* IEEE.
<https://doi.org/10.1109/PEMC61721.2024.10726347>

Important note

To cite this publication, please use the final published version (if applicable).
Please check the document version above.

Copyright

Other than for strictly personal use, it is not permitted to download, forward or distribute the text or part of it, without the consent of the author(s) and/or copyright holder(s), unless the work is under an open content license such as Creative Commons.

Takedown policy

Please contact us and provide details if you believe this document breaches copyrights.
We will remove access to the work immediately and investigate your claim.


Green Open Access added to TU Delft Institutional Repository


'You share, we take care!' - Taverne project


<https://www.openaccess.nl/en/you-share-we-take-care>


Otherwise as indicated in the copyright section: the publisher is the copyright holder of this work and the author uses the Dutch legislation to make this work public.

Investigating the Effect of Power Curtailment on the Switch of a Solar Boost Converter Under Residential Loads

Joel Alpízar-Castillo
Delft University of Technology
Delft, The Netherlands
J.J.AlpizarCastillo@tudelft.nl 

Carina Engström
Delft University of Technology
Delft, The Netherlands
C.B.M.Engstrom@tudelft.nl 

Laura Ramírez-Elizondo
Delft University of Technology
Delft, The Netherlands
L.M.RamirezElizondo@tudelft.nl 

Pavol Bauer
Delft University of Technology
Delft, The Netherlands
P.Bauer@tudelft.nl 

Abstract—The massive deployment of PV systems in residential buildings is causing voltage challenges in low-voltage distribution networks. Worldwide, DSOs started requesting users to curtail power when this is injected back into the grid. Although many commercially available inverters can perform curtailment, the degradation effects of curtailment still have to be investigated. This paper estimated how power curtailment affects the reliability of a boost converter working below MPPT voltages. Using the mission profile method, we determined the conduction and switching losses on the converter switch as the critical component, based on its temperature and current profiles. The results suggest that curtailing the power requires the operation point to move towards lower PV voltages, leading to deeper thermal cycles, therefore reducing the expected lifetime of the converter by up to 80 % for power injection into the grid below 1.5 kW. From the operational perspective, this might require premature replacements compared to operating under MPP conditions, affecting the revenue forecast before the enforcement of curtailment. For power injection above 1.5 kW, the LCoE does not change compared to the case without considering the degradation. However, near zero-injection conditions, the difference in LCoE between considering and not considering replacements increases exponentially up to 135 %.

Index Terms—Boost converter, Power Curtailment, Power Electronics Degradation, Reliability

I. INTRODUCTION

Modern power systems are migrating from traditional rotational energy sources to power electronic-controlled devices. The share of renewable energy sources (RES) increases year-to-year, urging distribution and transmission system operators (DSOs and TSOs, respectively) to adapt their systems to their stochastic behaviour. At the low-voltage distribution level, DSOs face the challenge of numerous distributed renewable

energy resources (DRES), mostly PV, installed throughout the network, compromising voltage stability. During peak generation, the DRES usually produces more energy than locally consumed in residential buildings, injecting the surplus into the grid and raising the voltage in those nodes.

To overcome this challenge, DSOs throughout the world have implemented different strategies. In some cases, the network infrastructure has been reinforced, requiring complex and expensive project planning and deployment. Nevertheless, this solution was insufficient due to the speed and cost at which the number of installations increased and the rate at which the grid is being reinforced [1]. Likewise, storage systems like BESS [2] and flywheels [3] have been used to compensate for power fluctuations, but the cost and complexity are still challenging. Alternatively, some local governments have entitled DSOs to request prosumers to curtail their power generation to cap the energy injected into the grid. The main argument is that those DRES systems should operate for self-consumption, not grid injection. In the Netherlands, curtailment is an essential assumption in the grid transformation plans for 2050 [4]. In the United Kingdom, the engineering recommendation EREC G100, by the Energy Networks Association (ENA), allows DSOs to limit their customer's energy import and export [1]. Similarly, Germany's Renewable Energy Sources Act EEG2012 sets the maximum feed-in power into the grid to 70 % of the installed DRES system capacity [5]. When prosumers do not have energy storage systems (EESs) available, they might need to curtail power to comply with those regulations.

Although many modern solar inverters can curtail power, the effect of operation outside the maximum power point (MPP) to follow curtail orders still has to be investigated. If the power electronics converter (PEC) continuously operates outside its nominal conditions, i.e., MPP, its reliability might be affected, leading to a different lifetime [6]. Some authors have studied the reliability of solar converters under

The project was carried out with a Top Sector Energy subsidy from the Ministry of Economic Affairs and Climate, carried out by the Netherlands Enterprise Agency (RVO). The specific subsidy for this project concerns the MOOI subsidy round 2020. Thanks to Miad Ahmadi, Aditya Shekhar, Faezeh Kardan, Siddhesh Shinde and Gautham Ram Chandra Mouli for collaborating on this work.

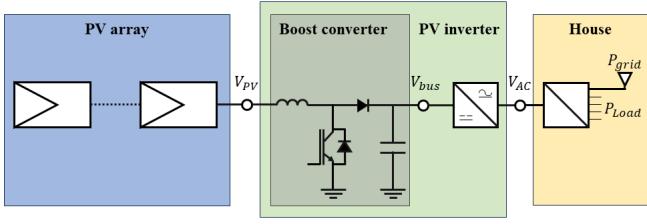


Fig. 1: Diagram of the considered system (PV array, inverter and house loads).

non-standard conditions to assess their effect on converter degradation. For example, [7] studied the reliability changes in solar inverters for sun-tracking PV systems, demonstrating that given the increased power the inverter has to handle, the total failure rate also increases. The impact of reactive power injection was studied in [8] and [9], evaluating the economic impact of the converter's lifetime reduction. All studies used the mission profile method. This way, there is a risk that enforced curtailment would affect the financial forecast not only on the energy lost but also would accelerate the inverter degradation, ultimately requiring an early replacement. The contributions of this work are:

- estimating, through a residential case scenario, the changes in the expected lifetime of the switch of a boost converter when operating in a voltage-controlled curtailment mode, and
- analysing the impacts on the levelized cost of energy caused by the accelerated degradation of a boost converter due to power curtailment on a residential case scenario.

II. SYSTEM MODEL

We studied a 2 kW PV array connected to a boost converter to supply power to a DC bus within a PV inverter, as shown in Fig. 1. In typical operation conditions, the switching pattern in the converter would ensure maximum power transfer; however, the power available could surpass the load, and the excess has to be injected into the grid, which could cause overvoltages. For that reason, given a signal, the converter would change from MPPT to curtailment mode. Changing the operation point has two effects. On the PV side, decreasing the power requires decreasing either the current or the voltage; nevertheless, they are mutually dependent; thus, changing the power output would change the voltage for the PV module, i.e., at the converter's input. On the converter side, a change in power is made by changing the duty cycle of the switch, therefore changing the time the switch and diode operate, as well as their currents. Although some components on the AC side, such as the DC link capacitor, are also affected by operating outside MPPT conditions, this work focuses on the boost converter.

A. PV model

Photo-voltaic modules are well-studied in the literature. We used the model in [10] for this work, as it considers the effects of temperature and irradiance for the current calculations. The

model describes the current as a function of the voltage V_{PV} , the irradiance G , and the temperature T given by

$$I(V_{PV}, G, T) = I_L(G, T) - I_0 \exp \left[\frac{q(V_{PV} + IR_s)}{nkT} - 1 \right], \quad (1)$$

with

$$I_L(G, T) = I_{L_{T_1}}(G) [1 + K_0(T - T_1)],$$

$$I_{L_{T_1}}(G) = \frac{G I_{SC_{T_1}}}{G_{ref}},$$

$$K_0 = \frac{I_{SC_{T_2}} - I_{SC_{T_1}}}{T_2 - T_1} \cdot 3$$

$$I_0 = I_{0(T_1)} \left(\frac{T}{T_1} \right)^{\frac{n}{\beta}} \exp \left[\frac{-qV_g}{nk} \left(\frac{1}{T} - \frac{1}{T_1} \right) \right],$$

$$I_{0(T_1)} = \frac{I_{SC_{T_1}}}{\exp \left(\frac{qV_{OC_{T_1}}}{nkT_1} - 1 \right)},$$

$$R_S = -\frac{dV_{PV}}{dI_{V_{OC}}} - \frac{1}{X_V}$$

$$X_V = I_{0(T_1)} \left(\frac{q}{nkT_1} \right) \exp \left(\frac{qV_{OC_{T_1}}}{nkT_1} \right)$$

where $I_{SC_{T_1}}$ and $V_{OC_{T_1}}$ are the short circuit current and open circuit voltage at the reference temperature T_1 (in this case 25 °C), respectively. The remaining constants are the elementary charge q , the ideality factor n , the Boltzmann's constant k , the voltage temperature coefficient β , the reference irradiance G_{ref} (in this case 1000 W/m²), and the band gap V_g . The manufacturer's datasheet provides these parameters.

B. Boost Converter

The degradation of any power electronics component depends on its utilization. For this reason, we need expressions for the currents on the critical components of the boost converter. In this work, we focused on the effects on the switch when power curtailment puts voltage constraint at the DC link, and assumed continuous conduction mode. The switching causes a change of voltage in the inductor to reverse its polarity. When the switch conducts, the current flows through it. Otherwise, the current flows through the diode to the load (see Fig. 2). The switch duty cycle D determines the power obtained from the PV array and transferred to the load. As the bus has a constant voltage V_{bus} and a current i_o , the analysis should focus on the current level. For the inductor, the average current \bar{i}_L is

$$\bar{i}_L = \frac{V_{bus} i_o}{V_{PV}}, \quad (2)$$

limited by

$$\begin{cases} i_{max} = \bar{i}_L + \frac{\Delta i_L}{2} = \frac{V_{bus} i_o}{V_{PV}} + \frac{V_{PV} D}{2 f_s L} \\ i_{min} = \bar{i}_L - \frac{\Delta i_L}{2} = \frac{V_{bus} i_o}{V_{PV}} - \frac{V_{PV} D}{2 f_s L} \end{cases} \quad (3)$$

Similarly, for the switch, the average current is

$$\bar{i}_S = \frac{D(i_{max} + i_{min})}{2} = \frac{V_{bus} i_o D}{V_{PV}}. \quad (4)$$

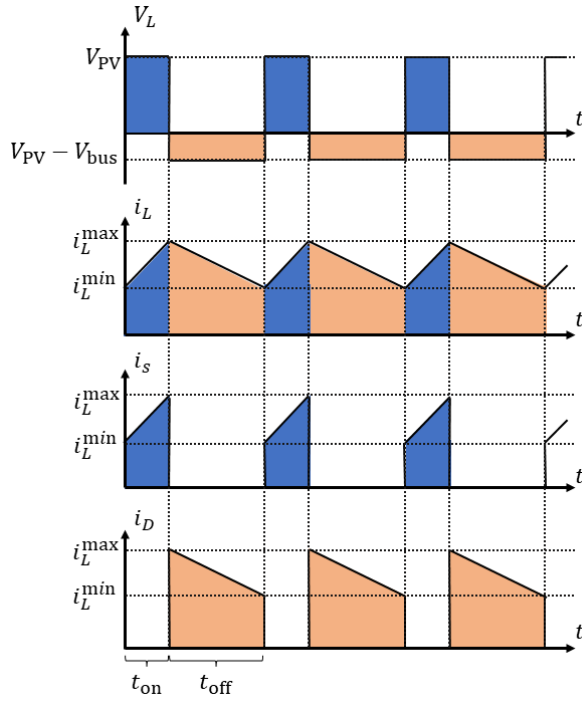


Fig. 2: Behaviour of the a) inductor voltage V_L , b) inductor current i_L , c) switch current i_s and d) diode current i_D in continuous conduction mode.

while the RMS current is

$$i_{s,RMS} = \sqrt{f_s \int_0^{t_{on}} \left[\frac{(i_{max} - i_{min})t}{t_{on}} + i_{min} \right]^2 dt} \quad (5)$$

$$= \sqrt{D \left[\left(\frac{V_{bus} t_o}{V_{PV}} \right)^2 + \frac{1}{3} \left(\frac{V_{PV} D}{2f_s L} \right)^2 \right]}$$

C. Switching Control

The operation of the converter will be governed by permitted power injection into the grid due to the imbalance between the load and the PV generation. In this work, we call the maximum permitted power to be injected in the grid at any time *curtailment threshold* P_{grid}^{min} (the convention considered for P_{grid} is positive when power is demanded from the grid). If no curtailment is needed, the duty cycle will ensure MPP conditions. However, when the power imbalance surpasses the curtailment threshold, the control will reduce the power extracted from the PV system by changing the duty cycle. At any moment, the time the switch is activated t_{on} is given by

$$t_{on}(P_{grid}) = \frac{V_{bus} - V_{PV}(P_{grid})}{f_s V_{bus}}, \quad (6)$$

where V_{bus} is the voltage at the DC bus, V_{PV} is the voltage from the PV array and f_s is the switching frequency.

One can either increase or decrease the maximum power point voltage to reduce the power extracted from a PV module, as shown in the characteristic I-V and P-V curves in Fig. 3. On the one hand, increasing the voltage would allow a wider curtailment range as the duty cycle is improved, given the inverse proportionality between V_{PV} and D , with a fixed V_{bus} .

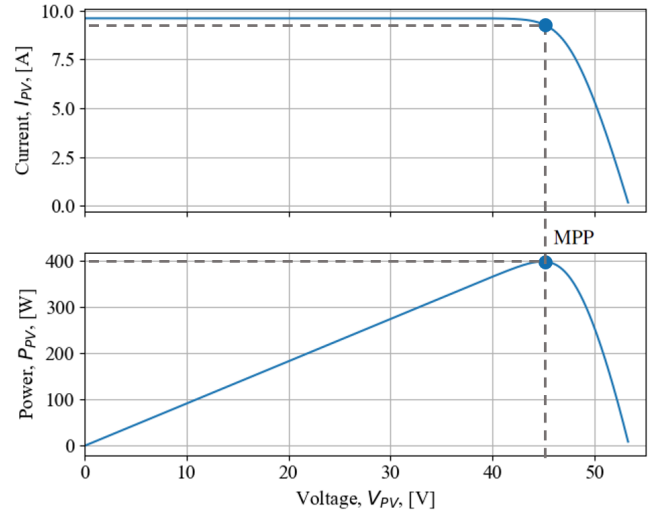


Fig. 3: I-V and P-V curves for the PV module considered in standard test conditions.

However, controlling the power in that range might be more complex due to the steep power decline when increasing the voltage above the MPP point [11]. On the other hand, reducing the power by reducing the voltage allows smoother control, but reduces the curtailment range as the duty cycle increases. Nevertheless, the curtailment is unlikely to reach 100 %. Normally, the load demands power from the PV system, and the DSO sets the curtailment threshold at the grid connection point. Thus, we considered the left side of the maximum power point to control the curtailment.

III. POWER LOSSES MODEL

Multiple methods can be used to estimate the expected life of power electronic devices. Among those, the mission profile and the military handbook are the most common [12]. For this work, we used the mission profile method, as it allows a more straightforward evaluation of different power profiles associated with different power curtailment levels. We will focus on the switch degradation. Following the method proposed by [13]; first, we determined the average and RMS currents in the switch as (4) and (5) respectively. For this work, we will use IGBTs as switches. Their conduction and switching losses per switching cycle are, respectively,

$$P_c(t) = V_s |\bar{i}| + R_{CE} i_{RMS}^2 \quad (7)$$

and

$$P_s = \frac{f_s E_s |V_s|}{V_{nom}} \quad (8)$$

where V_s and V_{nom} are the instantaneous voltage and nominal voltage for test conditions, respectively, and R_{CE} is the collector-emitter resistance. The turn-on energy loss given by

$$E_s = a_T + b_T |\bar{i}| + c_T i_{RMS}^2 \quad (9)$$

where a_T , b_T , and c_T are dynamic characteristic parameters that can be obtained from the datasheet. This way, the total power losses are

$$P_{T,s} = P_c + P_s. \quad (10)$$

TABLE I: Parameters used in Bayerer's lifetime model.

Symbol	Parameter	Value	Unit
<i>IGBT model: STGB5H60DF</i>			
A	IGBT technology factor	9.34×10^{14}	-
β_1	-	-4.416	-
β_2	-	1285	-
β_3	-	-0.463	-
β_4	-	-0.716	-
β_5	-	-0.761	-
β_6	-	-0.5	-
I	Current per bond foot	10	A
V	Voltage class	6	-
d	Bond wire diameter	450	μm

The junction temperature can be calculated as a function of the total power losses and the ambient temperature T_a using

$$T_S = P_T Z_{j-c} + T_a. \quad (11)$$

The thermal impedance between the junction and the case, Z_{j-c} , can be calculated by the Foster method as

$$Z_{j-c} = \sum_{i=1}^n \left(\lim_{t \rightarrow \infty} R_i \left[1 - \exp\left(-\frac{t}{\tau_i}\right) \right] \right) \quad (12)$$

Where R_i and τ_i are the equivalent thermal resistances provided by the manufacturer.

Following the recommendations in [14], we used the Bayerer method to estimate the end of life of the switches. The thermal cycles to failure are given by

$$N_f = A \Delta T_j^{\beta_1} \exp\left(\frac{\beta_2}{T_j^{\min}}\right) t_{on}^{\beta_3} I_b^{\beta_4} V^{\beta_5} d^{\beta_6}, \quad (13)$$

where ΔT_j is the j -th thermal cycle, T_j^{\min} is the minimum junction temperature (in kelvin) at the j -th thermal cycle, t_{on} is the on-time, I_b is the current per band wire, V is the voltage, d is the diameter of the bonding wire, and A and β_i are constants given by the method, shown in Table I.

A method for cycle counting is required to determine the combinations of ΔT_j and T_j^{\min} for each cycle to failure N_f . Rainflow counting is often used in this context [15], allowing us to estimate the accumulated damage D caused per cycle to failure as

$$D = \sum_{j=1}^m \frac{n_j}{N_{f,j}}, \quad (14)$$

where n_j is the total number of thermal cycles with the conditions in (13).

IV. COST ESTIMATIONS

Most users' main incentive for acquiring a PV system is to reduce energy costs [16]. Such savings are often determined by comparing the PV system's levelized cost of energy (LCoE) against the price of the energy purchased from the grid. The lower the PV system LCoE, the bigger the revenue. This way, the LCoE is a function of the total cost and energy generation of the system during a period of n , given by

$$LCoE = \frac{CAPEX + \sum_{i=1}^n \left[\frac{OPEX_i}{(1+r)^i} \right]}{\sum_{i=1}^n E_i} \quad (15)$$

where the CAPEX is the capital expense of the project, i.e., the up-front cost of the system, the OPEX are the project's

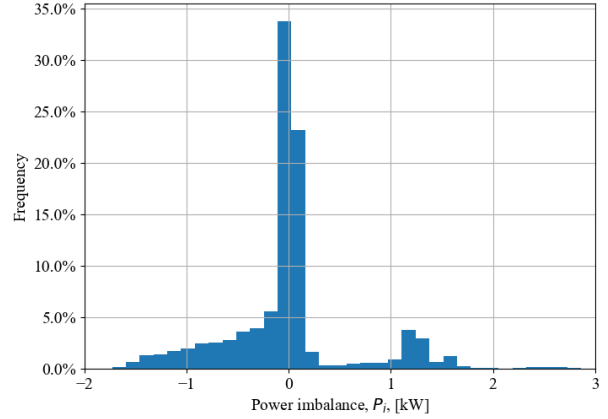


Fig. 4: Power imbalance between the load and the PV generation without curtailment.

operational costs, and r is the discount rate. Given their size, residential PV systems rarely have operational costs beyond component replacement, mostly due to external factors (e.g., weather or manufacturing defects). Therefore, we considered the inverter replacements as operational costs due to the shortening in the converter's life caused by the curtailment (we assumed that the inverters cannot be repaired if the converter fails). Also, we considered a linear PV generation decrease of 20 % in 25 years to estimate the yearly energy production E_i in (15).

V. RESULTS AND DISCUSSION

The proposed case scenario to evaluate the power curtailment effect on the boost converter switch comprises a residential PV system of five 400 W modules connected in series. The load is generated using a probabilistic generator, using the probabilities and power for different appliances [17], the distribution of the power imbalance between the load and the PV generation without curtailment is shown in Fig. 4. The parameters used for the simulation are shown in Table II. From (6), one can notice that the lower voltages resulting from different curtailment thresholds will decrease the duty cycle despite increasing the maximum current. This is reflected in lower currents flowing through the switch. Note that such lower currents will occur only when the converter is not operating in MPPT mode but in curtailment. Thus, a sudden curtailment requirement will produce a deeper thermal cycle ΔT , since the junction temperature is proportional to the current, as per (7) - (11).

The previous effect is demonstrated in Fig. 5, where we show the current and mission profile for two days, one in winter and one in summer. Curtailing in summer is more frequent; higher irradiance requires the converter to reduce more power output as the curtailment threshold moves towards a zero-injection scenario, reducing the voltage and increasing the ΔT . When this effect is studied for the full range of curtailment thresholds in the case scenario, it becomes apparent that

TABLE II: Parameters used in the simulation.

Symbol	Parameter	Value	Unit
<i>PV module</i>			
V_{OC}	Open circuit voltage	53.4	V
I_{SC}	Short circuit current	9.60	A
V_{MPP}	MPP voltage	44.1	V
I_{MPP}	MPP current	9.08	A
β	Voltage temperature coefficient	-0.29	%/°C
V_g	Band gap	1.79×10^{-19}	J
n	Ideality factor	1.4	-
<i>Boost converter</i>			
V_{bus}	Bus voltage	400	V
f_s	Switching frequency	20	kHz
L	Inductance	1.45	mH
<i>IGBT model: STGB5H60DF</i>			
V_T	Terminal collector-emitter voltage	1.198	V
R_{CE}	Collector-emitter resistance	00856	Ω
a_T	-	0.0195	W-s
b_T	-	0.011	V-s
c_T	-	0.0005	Ω
V_{nom}	Testing nominal voltage	600	V
$R_{j-c,i}$	Junction-case thermal resistance	1.7	°C/W
$R_{c-h-a,i}$	Case-ambient thermal resistance	8	°C/W

curtailment thresholds closer to 0 will have more and deeper thermal cycles, as shown in Fig. 5. This directly affects the component's lifetime, as shown in Fig. 6.

Similarly, the converter's lifetime depends on its components. By assuming a direct proportionality between the converter and switch lifetime, we estimated the replacement year by normalising the replacement year to the case without curtailment. Fig. 6 suggests that actively curtailing the power will lead to early replacements. This would drastically affect the forecasted revenue of the system, as inverters can account for up to a third of the total cost of a residential PV system. Note that this assumption is, in fact, optimistic, as we are not including the other components in this work, namely the diode and the capacitor, which would likely have similar thermal responses to the power curtailment.

We can now analyse the changes in the LCoE, considering the estimated replacement dates for the different curtailment thresholds. We estimated the LCoE for each curtailment threshold using (15), with a period of 25 years, a discount rate of 8 %, and an initial investment of €4 000. For the inverter, we considered a replacement cost of €1 250 (equipment and labour) and an expected base lifetime of 15 years [18]. In Fig. 7, we presented two cases for the LCoE: one without considering the early replacement due to accelerated degradation caused by the power curtailment (taken as the base case) and one considering the replacement costs, demonstrating a clear increment in the LCoE when the replacement costs are considered. In this case scenario, the homogenous behaviour of curtailment thresholds above 1.5 kW is explained by the load distribution shown in Fig. 4. As can be seen, the power injected back to the grid has lower occurrences above 1.5 kW; therefore, the system's behaviour is expected to remain constant in that range, being the LCoE that considers the replacements equal to the base case. The demand increases for values closer to zero-injection; thus, the system has to curtail power more frequently the closer the

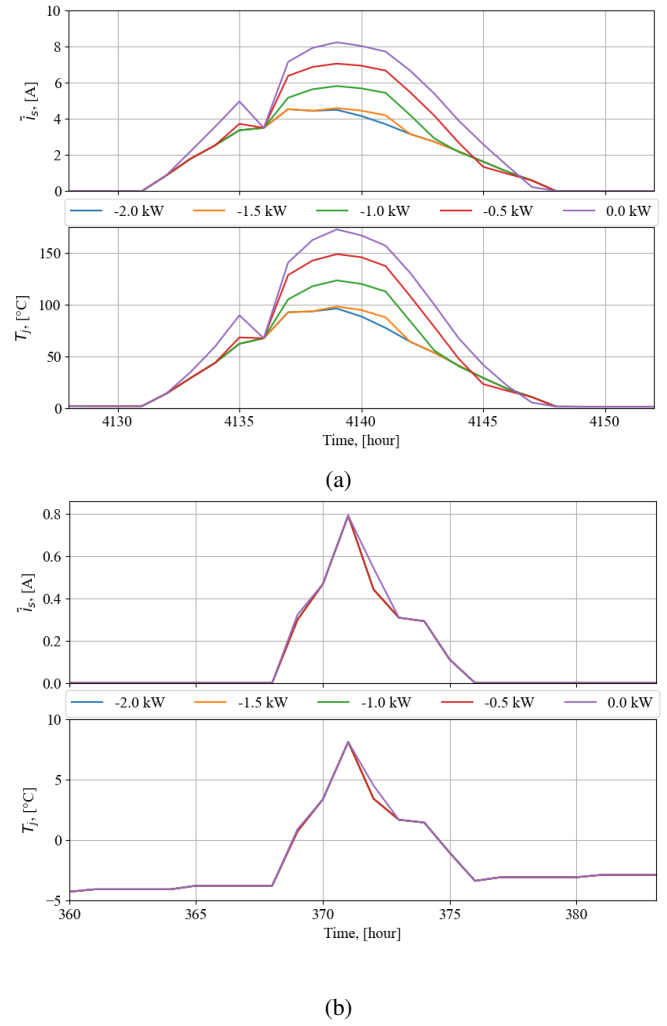


Fig. 5: Representative behaviour of the average current and junction temperature during a) summer and b) winter for different curtailment thresholds.

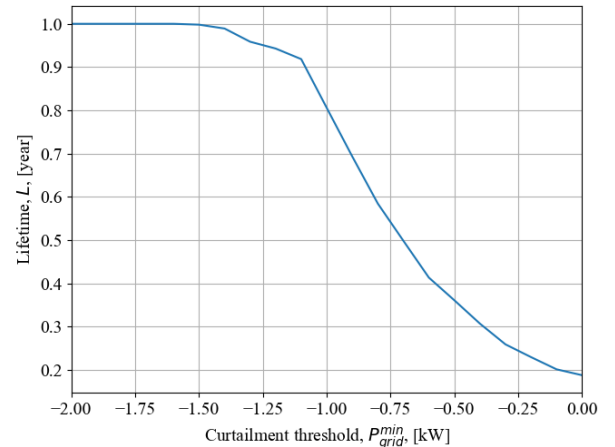


Fig. 6: Normalized expected lifetime of the switch per curtailment threshold.

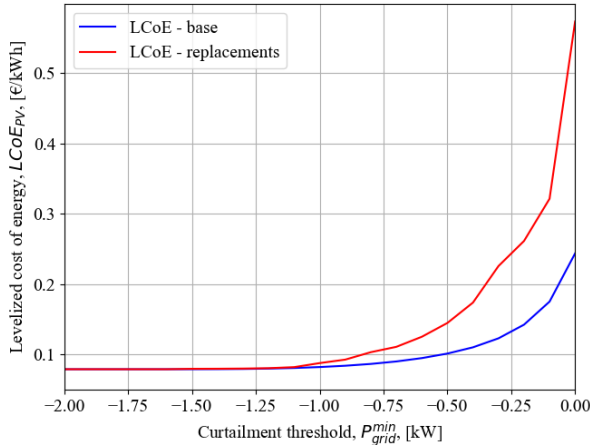


Fig. 7: LCoE for different curtailment thresholds.

threshold is to 0 kW. This directly impacts the switches, as the current and junction temperature increase, leading to an exponential increment in the LCoE to over 135 % of the base case, increasing from 0.244 €/kWh to 0.573 €/kWh. For these ranges, turning off the inverter completely could be an option, but a control strategy considering the degradation of the device would be required.

VI. CONCLUSIONS

This work analyzed the degradation and cost effects enforced power curtailment has on the converter of a PV system in a residential case scenario. Considering a boost converter, we investigated the change in the lifetime of an IGBT switch as the component most likely to fail, thus urging a replacement of the inverter. From a degradation perspective, curtailment thresholds closer to 0 kW decreased the voltage on the converter's input. Lower input voltages required lower duty cycles and sudden changes to lower currents. Those sudden current changes resulted in more frequent and deep thermal cycles, ultimately leading to an early failure, compared with the case without curtailment for thresholds below 1.5 kW, reducing the expected component lifetime by up to 80 % in the zero-injection scenario. Then, assuming a correlation between the lifetime of the switch and the converter (thus, the inverter), we suggested a behaviour for the levelized cost of energy considering an early replacement. Compared with the case without considering the degradation of the components, the levelized cost of energy of the overall system remains constant for power curtailment thresholds above 1.5 kW. Below, the LCoE increased exponentially by up to 135 % at the zero-injection condition. This way, for residential use, power curtailment thresholds that allow injecting up to 1.5 kW into the grid will not negatively affect the LCoE of the system. However, enforcing curtailment without compensation can lead to unprofitable scenarios.

REFERENCES

- [1] "Technical requirements for customers' export and import limitation schemes," Energy Networks Association, Engineering Recommendation G100 Issue 2 2022 Amendment 2, April 2023. [Online]. Available: [https://www.energynetworks.org/assets/images/ENA_EREC_G100_Issue_2_Amendment_2_\(2023\).pdf](https://www.energynetworks.org/assets/images/ENA_EREC_G100_Issue_2_Amendment_2_(2023).pdf)
- [2] M. Stecca, L. R. Elizondo, T. B. Soeiro, P. Bauer, and P. Palensky, "A comprehensive review of the integration of battery energy storage systems into distribution networks," *IEEE Open Journal of the Industrial Electronics Society*, vol. 1, pp. 46–65, 2020.
- [3] S. Karrari, M. Noe, and J. Geisbuesch, "High-speed flywheel energy storage system (fess) for voltage and frequency support in low voltage distribution networks," in *2018 IEEE 3rd International Conference on Intelligent Energy and Power Systems (IEPS)*, 2018, pp. 176–182.
- [4] "2020-2050 Integrated Infrastructure Outlook," TenneT, Tech. Rep. II3050, October 2023. [Online]. Available: https://tennet-drupal.s3.eu-central-1.amazonaws.com/default/2023-10/II3050_Eindrapport.pdf
- [5] "Export limitation," SolarEdge, Application Note Version 2.8, March 2022. [Online]. Available: https://knowledge-center.solaredge.com/sites/kc/files/feed-in_limitation_application_note.pdf
- [6] S. Nyamathulla, D. Chittathuru, and S. M. Muyeen, "An overview of multilevel inverters lifetime assessment for grid-connected solar photovoltaic applications," *Electronics*, vol. 12, no. 8, 2023.
- [7] A. Azizi, S. Peyghami, S. F. Zarei, and F. Blaabjerg, "The impact of sun tracking on the reliability of solar inverters," in *2022 International Power Electronics Conference (IPEC-Himeji 2022- ECCE Asia)*, 2022, pp. 1553–1559.
- [8] S. S. Kshatri, D. S. N. M. Rao, P. C. Babu, D. G. Kumar, and N. V. Sireesha, "Reliability evaluation of pv inverter considering impact of reactive power injection," in *2022 IEEE 2nd International Conference on Sustainable Energy and Future Electric Transportation (SeFeT)*, 2022, pp. 1–5.
- [9] A. Anurag, Y. Yang, and F. Blaabjerg, "Impact of reactive power injection outside feed-in hours on the reliability of photovoltaic inverters," in *2015 IEEE 6th International Symposium on Power Electronics for Distributed Generation Systems (PEDG)*, 2015, pp. 1–8.
- [10] J. Gow and C. Manning, "Development of a model for photovoltaic arrays suitable for use in simulation studies of solar energy conversion systems," in *1996 Sixth International Conference on Power Electronics and Variable Speed Drives (Conf. Publ. No. 429)*, 1996, pp. 69–74.
- [11] V. Paduani and N. Lu, "Implementation of a two-stage pv system testbed with power reserves for grid-support applications," in *2021 North American Power Symposium (NAPS)*, 2021, pp. 1–6.
- [12] M. Ahmadi, F. Kardan, A. Shekhar, and P. Bauer, "Reliability assessment of modular multilevel converters: A comparative study of mil and mission profile methods," in *International Conference on Integrated Power Electronics Systems CIPS 2024*, 2024.
- [13] R. Bayerer, T. Herrmann, T. Licht, J. Lutz, and M. Feller, "Model for power cycling lifetime of igbt modules - various factors influencing lifetime," in *5th International Conference on Integrated Power Electronics Systems*, 2008, pp. 1–6.
- [14] F. Kardan, A. Shekhar, and P. Bauer, "Quantitative comparison of the empirical lifetime models for power electronic devices in ev fast charging application," in *2023 11th International Conference on Power Electronics and ECCE Asia (ICPE 2023 - ECCE Asia)*, 2023, pp. 3239–3244.
- [15] S. S. Kshatri, J. Dhillon, and S. Mishra, "Impact of solar irradiance and ambient temperature on pv inverter reliability considering geographical locations," *International Journal of Heat and Technology*, vol. 39, no. 1, p. 292 – 298, 2021.
- [16] F. Penizzotto, R. Pringles, and F. Olsina, "Real options valuation of photovoltaic power investments in existing buildings," *Renewable and Sustainable Energy Reviews*, vol. 114, p. 109308, 2019.
- [17] M. Pipattanasomporn, M. Kuzlu, S. Rahman, and Y. Teklu, "Load profiles of selected major household appliances and their demand response opportunities," *IEEE Transactions on Smart Grid*, vol. 5, no. 2, pp. 742–750, 2014.
- [18] Bucher, Christof, Wandel, Jasmin, and Joss, David, "Life expectancy of pv inverters and optimizers in residential pv systems," in *WCPEC-8: EU PVSEC Proceedings*, 2022.